Biodistribution and Dosimetry of Technetium-99m-Hydrazino Nicotinamide IgG: Comparison with Indium-111-DTPA-IgG

Ronald J. Callahan, Sandra A. Barrow, Michael J. Abrams, Robert H. Rubin and Alan J. Fischman

Division of Nuclear Medicine, Department of Radiology, and Clinical Investigation Unit of the Medical Service, Massachusetts General Hospital; Departments of Radiology and Medicine, Harvard Medical School, Boston, Massachusetts; and Johnson Matthey Pharmaceutical Research, West Chester, Pennsylvania

The biological behavior of human polyclonal immunoglobulin G (IgG), radiolabeled with ^{99m}Tc via a nicotinyl hydrazine derivative (^{99m}Tc-HYNIC-IgG), was evaluated in normal human subjects. **Methods:** Initial biodistribution and dosimetry studies were performed in six normal male volunteers. Additionally, ^{99m}Tc-IgG and ^{111}In-DTPA-IgG were co-injected into six subjects and scintillation camera images were acquired at 6 and 18 hr later and serial blood and urine samples were collected. Biodistribution of both radiopharmaceuticals were measured by region of interest analysis. In the dual-injection group, images were crossover-corrected. **Results:** All subjects tolerated injection of the radiolabeled IgG preparations without apparent ill effects. Biodistribution of the two antibody preparations were remarkably similar with an increase in liver and abdominal activity for the ^{111}In preparation. Linear correlation of the tissue-to-blood ratios of ^{99m}Tc and ^{111}In-labeled IgG was observed at both times ($r^2 > 0.98$). The slopes of the regression line were 0.97 and 0.76 at 6 and 18 hr, respectively. The beta phase of the blood clearance of ^{99m}Tc-HYNIC-IgG was significantly delayed ($p < 0.01$) compared with ^{111}In-IgG ($t_{1/2}$: 51.9 ± 6.5 versus 35.3 ± 3.4 hr). In contrast, the volumes of distribution and urinary excretions of the radiopharmaceuticals were not significantly different. **Conclusion:** These studies establish that the biodistribution of ^{99m}Tc-HYNIC-IgG in normal human subjects is nearly identical to ^{111}In-DTPA-IgG.

Key Words: technetium-99m-HYNIC-IgG; indium-111-DTPA-IgG; dosimetry

J Nucl Med 1996; 37:843–846

Indium-111-labeled human polyclonal IgG has been demonstrated to be a useful radiopharmaceutical for imaging focal sites of inflammation in both animal models of infection and in human subjects (*1–3*). The mechanism of ^{111}In-IgG localization was originally postulated to involve binding of the Fc portion of the IgG to specific receptors on inflammatory cells (*1*). Microautoradiography studies, however, revealed that there is minimal association of radiolabel with inflammatory cells (*4*). In addition, it was recently demonstrated that although digestion of IgG with endoglycosidase-F significantly reduces Fc receptor binding, inflammation imaging is not altered (*5*). These observations suggest that inflammation localization is probably mediated by less specific mechanisms. It appears that nonspecific protein leak into the expanded protein space of inflammatory lesions plays an important role in the localization of ^{111}In-IgG (*6*). Since, diffusion of IgG into this expanded protein space occurs rapidly, early lesion detection should be possible if high-count density images are acquired. Unfortunately, the limited photon flux of the usual administered doses of ^{111}In-IgG makes it difficult to image the early stage of this process, due to the long acquisition times required to record a sufficient count density. A ^{99m}Tc-labeled IgG preparation could potentially solve this problem.

Recently, we reported that ^{99m}Tc-IgG prepared by a method using the hydrazino nicotinamide derivative of IgG (*7*) has nearly identical biodistribution and inflammation imaging properties to ^{111}In-IgG in rats (*7*), rabbits (*8*) and monkeys (*9*). Other work (*10*) comparing ^{99m}Tc-IgG prepared by the iminothiolane method (*11*) has shown lower infected muscle-to-gastrointestinal ratios with this formulation compare to ^{111}In-DTPA-IgG. In the present investigation, the imaging properties of ^{99m}Tc-hydrazino nicotinamide IgG were studied in normal human subjects.

MATERIALS AND METHODS

Subjects

Twelve normal male volunteers (aged 23–61 yr) were studied. All subjects had a complete medical history prior to participation in the study. A complete physical examination was performed prior to participation in the study and 1 wk later. The following laboratory studies were performed within 1 wk before radiopharmaceutical injection and 1 wk after study completion: hemoglobin, hematocrit, RBC count, WBC count with differential, platelet count, BUN, creatinine, SGOT, LDH, alkaline phosphatase and urine analysis. Vital signs (pulse, blood pressure and respiration rate) were measured before injection at 15-min intervals for the first hour, at 30-min intervals for the next 2 hr and at 6 and 24 hr.

The human studies protocol was approved by the Subcommittees on Human Studies, Radiation Safety and Pharmacy of the Massachusetts General Hospital. All subjects gave informed consent prior to participation.

Indium-111-Labeled IgG

Human polyclonal IgG radiolabeled with ^{111}In according to a previously described DTPA-carboxycarbonic anhydride chelate method (*12,13*) was used to produce this formulation. Approximately two DTPA groups were present per IgG. Radiochemical purity was determined using ITLC-SG chromatographic strips (Gelman Laboratories Ann Arbor, MI) developed with 0.1 *M* sodium citrate (pH 5.5). In the preparations used in the present studies, >90% of the radioactivity was associated with antibody.

Technetium-99m-Labeled IgG

Hydrazino nicotinamide derivatized IgG (HYNIC-IgG) was prepared by a previously reported method (*7*). The modified IgG used in the imaging studies had ~2.6 nicotinyl hydrazine groups/IgG. HYNIC-IgG was radiolabeled with ^{99m}Tc by addition of 20 mCi ^{99m}Tc-glucoheptonate to 0.5 ml (2.5 mg) of a solution of the derivatized protein. The mixture was incubated for 60 min at room temperature and radiochemical purity was determined as described above for ^{111}In-IgG. In the IgG preparations used in the present studies, >90% of the radioactivity was associated with antibody.

Received Feb. 6, 1995; revision accepted Oct. 8, 1995.

For correspondence or reprints contact: Alan J. Fischman, MD, Division of Nuclear Medicine, Department of Radiology, Massachusetts General Hospital, 32 Fruit St., Boston, MA 02114.

TABLE 1
Whole-Body and Organ Biodistribution of Technetium-99m-HYNIC-IgG (% Initial Whole-Body Activity)

Organ	Time (hr) 0	1	6	24
Whole Body	100	103 (1.7)	99.7 (1.3)	106 (3.7)
Lungs	3.7 (0.3)	3.0 (0.08)	2.7 (0.2)	2.2 (0.16)
Kidneys	1.4 (0.3)	1.3 (0.12)	1.4 (0.16)	1.5 (0.2)
Liver	8.0 (0.5)	8.2 (0.24)	7.8 (0.32)	9.0 (0.8)
Spleen	1.4 (0.3)	1.3 (0.2)	1.1 (0.16)	1.0 (0.24)
Heart	4.1 (0.4)	3.9 (0.40)	3.3 (0.4)	2.7 (0.20)

Data are mean (s.e.m.) for six subjects.

TABLE 3
Radiation Dosimetry of Technetium-HYNIC-IgG and Indium-111-DTPA-IgG in Human Subjects

Organ	rads/mCi ^{99m}Tc-HYNIC-IgG	^{111}In-DTPA-IgG*
Lung	0.029	0.649
Liver	0.042	1.42
Spleen	0.045	0.753
GI tract	0.022	0.45
Kidney	0.037	0.727
Muscle	0.018	0.48
Total body	0.019	0.467

*From Macroscint® Clinical Imaging Guide, McNeil Pharmaceutical, Springhouse, PA.

Imaging

Normal Human Biodistribution and Radiation Dosimetry Estimates for Technetium-99m-HYNIC-IgG. After intravenous injection of 20 mCi ^{99m}Tc-HYNIC-IgG (2.5 mg HYNIC-IgG) in six normal male volunteers aged 23–58 yr, anterior and posterior whole-body images were obtained immediately and at 6 and 24 hr postinjection using a large field of view gamma camera equipped with a parallel-hole, high-resolution collimator interfaced to a dedicated computer system. A 20% window centered around the 140-keV photopeak of ^{99m}Tc was used. Regions of interest (ROIs) were constructed at each time point for the whole body and all organs visualized. The geometric mean of activity in these regions was calculated and corrected for radioactive decay. Organ radioactivity, as a fraction of the administered dose, was calculated by using the immediate whole body as 100% of the injected dose. Serial urine and feces (n = 3) samples were collected and the radioactivity content determined.

From the imaging results, the residence time for ^{99m}Tc-HYNIC-IgG in the major source organs (heart chambers, kidneys, liver, lungs, spleen, urinary bladder contents (4-hr void) and the remainder whole body) was calculated and entered into the MIRDOSE2® computer program (*14*). Assumptions included instantaneous organ uptake, no biological clearance from source organs and a dynamic bladder model using a 4-hr voiding interval.

Dual Injection of Technetium-99m-HYNIC-IgG and Indium-111-DTPA-IgG. Another group of six subjects were injected with 10 mCi ^{99m}Tc-HYNIC-IgG (~2.5 mg protein) and 1.0 mCi ^{111}In-DTPA-IgG (~0.60 mg protein). Immediately after injection and at 6 and 18–24 hr later, whole-body scintigrams were acquired using a large field of view gamma camera equipped with a parallel-hole, medium-energy collimator interfaced to a dedicated computer system. Indium-111 and ^{99m}Tc images were acquired sequentially with 15% windows centered on photopeaks at 140 keV for ^{99m}Tc and 247 keV for ^{111}In. Venous blood samples (5 ml) were collected at 5, 10, 15 and 30 min and 1, 6 and 24 hr. Urine samples were collected over the following intervals: 0–2 hr, 2–6 hr and 6–24 hr.

Phantom studies were performed to calculate the amount of crossover of 174 keV photons of ^{111}In into the ^{99m}Tc window. Briefly, at the time that the subjects were injected, samples of ^{111}In-DTPA-IgG and ^{99m}Tc-HYNIC-IgG were thoroughly mixed with 250 ml saline in separate standard infusion bags in the same activity ratio as that injected into the subjects. At 6 and 18 hr later, the phantoms were placed 5 cm apart on the imaging table and images in both windows were acquired. From ROIs drawn around each bag, crossover factors were calculated. These factors were used to correct the ^{99m}Tc and ^{111}In images.

ROIs were drawn over the cardiac blood pool, lung, liver, spleen, kidney, intestine, bone and muscle, and radioactivity (cpm)/pixel was calculated. The blood clearance rate was determined by nonlinear least squares testing. Volumes of distribution were calculated by standard methods (*15*). The results were expressed as tissue-to-blood-pool background ratios.

Statistical Analysis

The results of the imaging studies were evaluated statistically by analysis of variance (ANOVA) followed by Duncan's new multiple range test (*16*). For each tissue, two-way ANOVA with a linear model with time after injection and radiopharmaceutical as classification variables was used: target-to-background ratios [T/B] = time + radiopharmaceutical + time × radiopharmaceutical. The

TABLE 2
Urinary and Fecal Excretion of Technetium-99m-HYNIC-IgG (% Administered Dose)

Subject no.	Urine 0–6 hr	6–24 hr	Total	Feces
1	4.3	3.8	8.2	0
2	2.5	2.4	4.9	—
3	1.9	4.6	6.5	—
4	5.0	1.7	6.7	1.2
5	0.15	24.2	24.3	1.3
6	4.2	2.7	6.9	0.004
Mean ± s.e.m.	3.0 ± 0.7	6.6 ± 3.2	9.6 ± 2.7	0.6

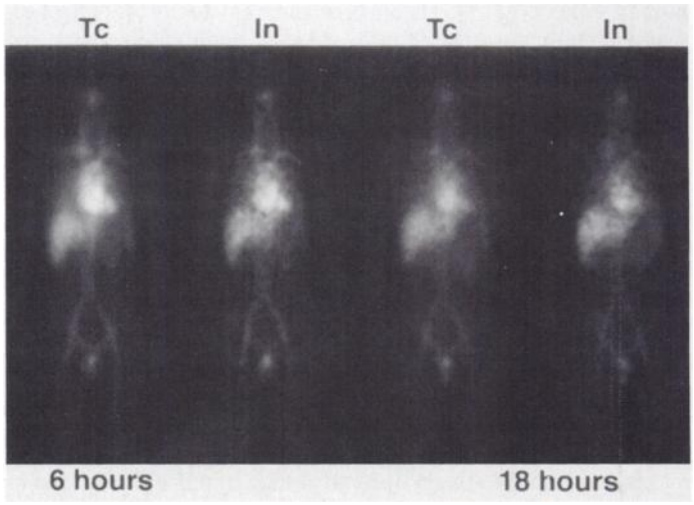

FIGURE 1. Anterior whole-body images of a normal human subject at 6 and 18 hr after injection of ^{99m}Tc-HYNIC-IgG and ^{111}In-DTPA-IgG. All images are normalized to the brightest pixel and corrected for crossover between the indium and technetium windows.

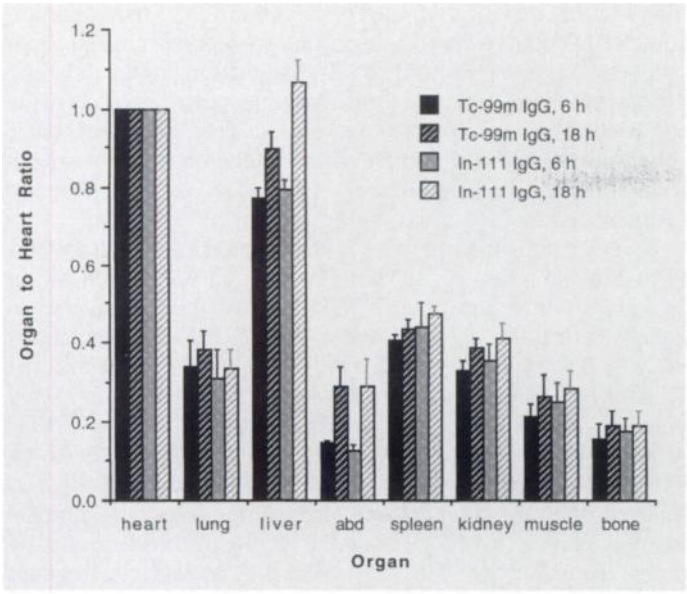

FIGURE 2. Biodistribution of ^{99m}Tc-HYNIC-IgG and ^{111}In-DTPA-IgG at 6 and 18 hr postinjection. Results are expressed as tissue-to-blood-pool accumulation ratios. Each point is the mean ± s.e.m. for six subjects.

first subscript of each F value is the number of degrees of freedom for the first classification variable (n − 1), the second classification variable (m − 1), the total for both classification variables (m + n − 2) or the interaction ((n − 1) × (m − 1)). The second subscript is the number of residual degrees of freedom (total number of observations − n × m). In addition, the target-to-background ratios for ^{111}In-IgG and ^{99m}Tc-IgG were compared by linear regression. All results were expressed as mean ± sem.

RESULTS

All subjects tolerated the intravenous administration of ^{111}In- and ^{99m}Tc-labeled IgG without apparent ill effects. Vital signs remained constant throughout the study and the pre- and poststudy laboratory values were indistinguishable.

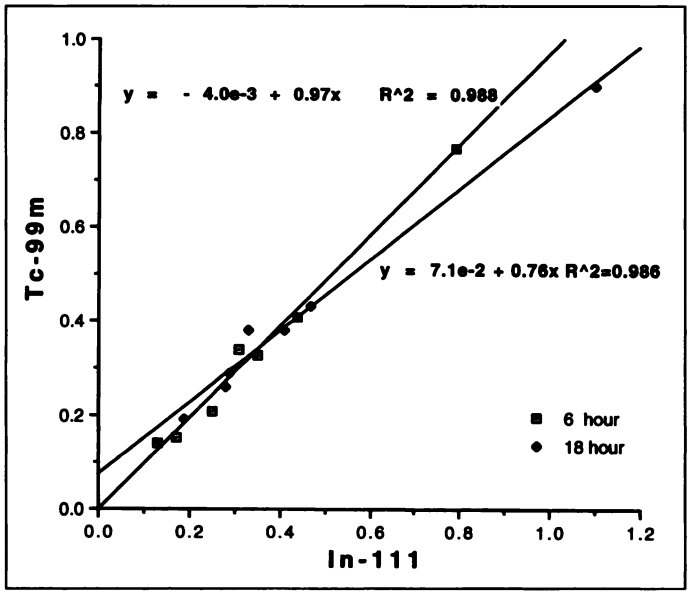

FIGURE 3. Tissue-to-blood ratios for ^{99m}Tc- and ^{111}In-labeled human polyclonal IgG at 6 and 18 hr postinjection. Slope and intercept of the regression lines were calculated to be: 6 hr T/B(^{99m}Tc) = 0.97*(T/B)^{111}In − 0.004 (r^2 = 0.988); 18 hr T/B(^{99m}Tc) = 0.76*(T/B)^{111}In + 0.071 (r^2 = 0.986).

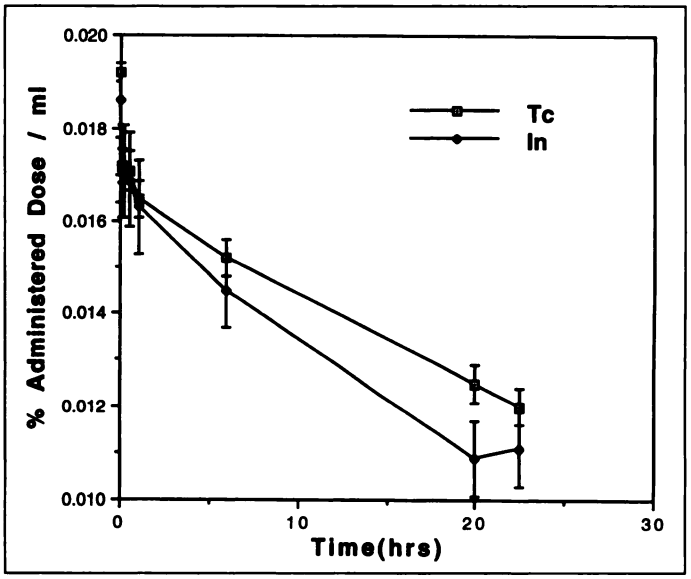

FIGURE 4. Blood time-activity curves for ^{99m}Tc-HYNIC-IgG and ^{111}In-DTPA-IgG. Each point is mean ± s.e.m. for six subjects.

Biodistribution and Radiation Dosimetry of Technetium-99m-HYNIC-IgG

Technetium-99m-HYNIC-IgG distributes primarily within the intravascular space. Results of organ ROI analysis are shown in Table 1.

Urinary and fecal excretion of ^{99m}Tc-HYNIC-IgG represents 9.6 ± 2.7% and 0.6% of the administered dose, respectively (Table 2).

Radiation absorbed dose estimates calculated from these data are shown in Table 3. For comparison, previously reported dosimetry data for ^{111}In-DTPA-IgG are included. These data support an adult dose of 20 mCi ^{99m}Tc-HYNIC-IgG, thereby providing a high photon flux with an acceptable radiation absorbed dose.

Dual Injections of Technetium-99m and Indium-111 IgG

The phantom studies indicated that at 6 hr after injection of the radiopharmaceuticals, ~5% of the photons detected in the ^{99m}Tc window were contributed by ^{111}In. At 18 hr postinjec-

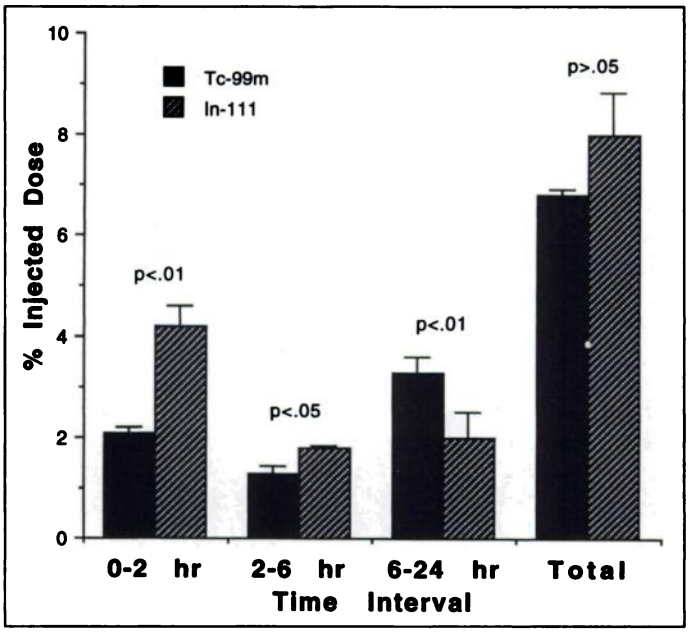

FIGURE 5. Fractional and total urinary excretion of ^{99m}Tc-HYNIC-IgG and ^{111}In-DTPA-IgG. Each point is mean ± s.e.m. for six subjects.

tion, ~17% of the photons detected in the ^{99m}Tc window were contributed by ^{111}In. At both imaging times, <2% of the photons detected in the ^{111}In window were contributed by ^{99m}Tc. All imaging data were corrected for spillover effects of ^{111}In into the ^{99m}Tc window.

Figure 1 shows representative, crossover-corrected, anterior whole-body images of a subject at 6 and 18 hr after co-injection of the radiolabeled IgG preparations. These images clearly demonstrate that the overall biodistribution of the two radiopharmaceuticals are nearly identical. At both imaging times, there were high concentrations of both radiopharmaceuticals in the cardiac blood pool, vascular structures, liver, spleen and kidney. Concentration of both tracers were lower in the lung, muscle, bone and gastrointestinal tract.

The biodistributions of ^{99m}Tc-HYNIC-IgG and ^{111}In-DTPA-IgG, expressed as tissue-to-blood-pool accumulation ratios at 6 and 18 hr postinjection are shown in Figure 2. ANOVA showed significant main effects of time after injection for liver ($F_{1,20}$ = 14.72, $p = 0.001$), abdomen ($F_{1,20}$ = 9.62, $p < 0.010$) and kidney ($F_{1,20}$ = 4.54, $p < 0.05$), but the main effects of the radiolabeling method and radiolabeling method by time interactions were not significant. The liver-to-blood-pool ratio of ^{111}In-DTPA-IgG at 18 hr after injection was greater than ^{99m}Tc-HYNIC-IgG ($p < 0.05$) and greater than both preparations at 6 hr ($p < 0.01$). Abdominal activity of ^{111}In-DTPA-IgG at 18 hr was greater than ^{99m}Tc-HYNIC-IgG and ^{111}In-DTPA-IgG at 6 hr ($p < 0.05$). The kidney-to-blood-pool ratio of ^{111}In-DTPA-IgG at 18 hr was greater than ^{99m}Tc-HYNIC-IgG at 6 hr ($p < 0.05$). For lung, spleen, muscle and bone, significant main effects of time, radiolabeling method or radiolabeling method by time interactions were not detected.

Results of regression analysis of tissue-to-blood ratios for ^{99m}Tc-and ^{111}In-labeled preparations are shown in Figure 3. The slope and regression line are calculated to be: 6 hr T/B(^{99m}Tc) = 0.97*(T/B) ^{111}In − 0.004 (r^2 = 0.988); 18 hr T/B(^{99m}Tc) = 0.76*(T/B) ^{111}In + 0.071 (r^2 = 0.986).

Figure 4 shows the blood time-activity curves for both radiopharmaceuticals. From these data, volumes of distribution were determined to be 6.1 ± 0.4 and 5.8 ± 13 liters for ^{99m}Tc-HYNIC-IgG and ^{111}In-labeled IgG (p = ns), respectively. In contrast, the beta phase of the blood clearance of ^{99m}Tc-HYNIC-IgG was significantly delayed ($p < 0.01$) compared with ^{111}In-DTPA-IgG ($t_{1/2}$: 51.9 ± 6.5 versus 35.3 ± 3.4 hr). Urinary excretion of the two IgG preparations is illustrated in Figure 5. Although significant differences were detected in the fractional excretion, the total 24-hr excretion for both preparations was not significantly different.

DISCUSSION

Radiolabeled human polyclonal IgG accumulates at sites of inflammation to a degree sufficient to yield excellent external images. This report compares the imaging properties of ^{99m}Tc-HYNIC-IgG to ^{111}In-DTPA-IgG in normal human subjects. The results clearly demonstrate the two different IgG preparations have similar imaging and biodistribution properties. The volumes of distribution and urinary excretions of the radiopharmaceuticals were also remarkably similar. In contrast, the beta phase of the blood clearance of ^{99m}Tc-HYNIC-IgG was significantly prolonged compared with ^{111}In-DTPA-IgG; similar results were observed in animal studies (*7*).

Although IgG radiolabeled with ^{99m}Tc by other methods has been used for infection/inflammation imaging, several significant problems exist with these preparations. First, these radiolabeled IgGs tend to clear from the circulation rapidly (*17*). Although this rapid clearance may result in favorable tissue-to-blood ratios, exposure of sites of infection to the radiopharmaceutical is decreased and imaging may be compromised. Second, due to possible antibody fragmentation in the labeling process, renal accumulation of tracer has been observed to be significantly increased (*17*). Third, and most important, these IgG preparations exhibit marked accumulation in the gastrointestinal tract, which significantly limits their use for evaluation of the abdomen (*10*).

Because clinical experience with ^{111}In-DTPA-IgG has demonstrated that most inflammatory lesions can be detected within 24 hr after injection (*1,2*), ^{99m}Tc-HYNIC-IgG should be an equally effective imaging agent. MIRDOSE 2 calculations indicate that approximately 20 mCi ^{99m}Tc-IgG can be injected without delivering a radiation burden in excess of 1 rad to any organ. Based on the physical properties of ^{111}In and ^{99m}Tc, nearly three-fold greater photon flux should be present at lesion sites at 18 hr postinjection if twentyfold more ^{99m}Tc-IgG is injected initially. In addition, due to the superior intrinsic imaging properties of ^{99m}Tc and the greater photon flux at early times, the technetium-labeled protein will provide much better quality images of infection sites, particularly if SPECT is used.

CONCLUSION

The results of this study establish that ^{99m}Tc-HYNIC-IgG and ^{111}In-DTPA-IgG have nearly identical biodistribution properties in normal humans. If these results can be generalized to patients with focal sites of infection or inflammation, the greater general availability and superior imaging properties of ^{99m}Tc may make this radiopharmaceutical an important agent for clinical imaging.

ACKNOWLEDGMENTS

This study was supported in part by a grant from the Robert Wood Johnson Pharmaceutical Research Institute, Raritan, NJ.

REFERENCES

1. Fischman AJ, Rubin RH, Khaw BA, et al. Detection of acute inflammation with ^{111}In-labeled nonspecific polyclonal IgG. *Semin Nucl Med* 1988;18:335–344.
2. Rubin RH, Fischman AJ, Callahan RJ, et al. Indium-111-labeled nonspecific immunoglobulin scanning in the detection of focal infection. *N Engl J Med* 1989;321:935–940.
3. Rubin RH, Fischman AJ, Nedelman M, et al. The use of radiolabeled, nonspecific polyclonal human immunoglobulin in the detection of focal inflammation by scintigraphy: comparison with gallium-67-citrate and technetium-99m-labeled albumin. *J Nucl Med* 1989;30:385–389.
4. Morrell EM, Tompkins RG, Fischman AJ, et al. An autoradiographic method for quantitation of radiolabeled proteins in tissue using indium-111. *J Nucl Med* 1989;30:1538–1545.
5. Fischman AJ, Fucello AJ, Pellegrino-Gensey JL, et al. Effect of carbohydrate modification on the localization of human polyclonal IgG at focal sites of bacterial infection. *J Nucl Med* 1992;33:1378–1382.
6. Juweid M, Strauss HW, Yaoito H, Rubin RH, Fischman AJ. Accumulation of immunoglobulin G at focal sites of infection. *Eur J Nucl Med* 1992;19:159–165.
7. Abrams MJ, Juweid M, tenKate CI, et al. Technetium-99m-human polyclonal IgG radiolabeled via the hydrazino nicotinamide derivative for imaging focal sites of infection in rats. *J Nucl Med* 1990;31:2022–2028.
8. Barrow SA, Graham W, Jyawook S, et al. Localization of ^{111}In-IgG, ^{99m}Tc-IgG, ^{111}In-labeled white blood cells at sites of acute bacterial infection in rabbits. *J Nucl Med* 1993;34:1975–1979.
9. Fischman AJ, Solomon HF, Babich JW, et al. Imaging of focal sites of inflammation in Rhesus monkeys with ^{99m}Tc-labeled human polyclonal IgG. *Int J Nucl Med Biol Part B* 1994;21:111–116.
10. Solomon HF, Oyen W, Abrams MJ, et al. Comparative studies of ^{111}In- and ^{99m}Tc-labeled polyclonal IgGs. International Symposium of Scintigraphic Detection of Infectious Disease, Nijmegen, The Netherlands; 1992:175–181.
11. Goedemans WT, Panek KJ. A new method for labeling proteins with ^{99m}Tc [Abstract]. *J Nucl Med All Sci* 1989;33:286.
12. Khaw BA, Mattis JA, Melincoff G, Strauss HW, Gold HK, Haber E. Imaging of experimental myocardial infarction. *Hybridoma* 1984;3:11–23.
13. Krejcarek GE, Tucker KL. Covalent attachment of chelating groups to macromolecules. *Biochem Biophys Res Commun* 1977;77:581–585.
14. Watson EE, Stabin M, Bolch WE. MIRDOSE 2 Computer Program. Oak Ridge Associated Universities. Oak Ridge, TN; 1984.
15. Gibaldi M, Perrier D. *Pharmacokinetics*, 2nd ed. New York: Marcel Dekker; 1982.
16. Duncan DB. Multiple range tests and multiple F-tests. *Biometrics* 1955;11:1–42.
17. Hnatowich DJ, Mardirossian G, Rusckowski M, Fogarasi M, Virzi F, Winnard P. Directly and indirectly technetium-99m-labeled antibodies—a comparison of in vitro and in vivo properties. *J Nucl Med* 1993;34:109–119.